



MONTCLAIR STATE
UNIVERSITY

Montclair State University
**Montclair State University Digital
Commons**

Theses, Dissertations and Culminating Projects

8-2021

Coastal Onlap/Offlap Amplification due to Organic Sediment Accumulation and Degradation : Implications for Sea Level Reconstruction

Norjmaa Khosbaatar
Montclair State University

Follow this and additional works at: <https://digitalcommons.montclair.edu/etd>



Part of the [Earth Sciences Commons](#), and the [Environmental Sciences Commons](#)

Recommended Citation

Khosbaatar, Norjmaa, "Coastal Onlap/Offlap Amplification due to Organic Sediment Accumulation and Degradation : Implications for Sea Level Reconstruction" (2021). *Theses, Dissertations and Culminating Projects*. 775.

<https://digitalcommons.montclair.edu/etd/775>

This Thesis is brought to you for free and open access by Montclair State University Digital Commons. It has been accepted for inclusion in Theses, Dissertations and Culminating Projects by an authorized administrator of Montclair State University Digital Commons. For more information, please contact digitalcommons@montclair.edu.

ABSTRACT

Coastal-plain depositional systems such as fluvial deltas are archives of past external (allogenic) forcing, such as sea-level variations, and their evolution can be described by two geomorphic boundaries: the alluvial-basement transition or upstream boundary, and the shoreline or downstream boundary. Patterns of landward/seaward migration of the shoreline (i.e., transgression/regression) and the alluvial basement transition (i.e., coastal onlap/offlap) in the rock record are often used for reconstruction of past sea-level changes. Theories for stratigraphic interpretation, however, need to be adapted to deal with internal (autogenic) processes that could play a significant role, but are to date largely unexplored. In particular, in-situ organic matter accumulation via plant growth has generally received little attention despite accounting for a significant volume fraction in most fluvio-deltaic plains and likely affect their response to sea level variations. To fill this knowledge gap, we develop a geometric model for the long-profile evolution of a fluvio-deltaic environment that accounts for sea-level cycles and organic sediment dynamics. The model assumes that sedimentological processes (i.e., inorganic and organic sedimentation) operate to preserve a linear geometry for both the delta plain or topset, and the subaqueous offshore region or forest. Changes in topset length can occur via shoreline transgression/regression, or coastal onlap/offlap, and the magnitude and timing of these changes can be directly related to the amplitude, phase and frequency of the sea-level variations. The model predicts that the maximum organic fraction occurs when the organic matter accumulation rate matches the accommodation rate, an observation consistent with field observations from coal geology. Further, we find that organic matter accumulation during the topset aggradation and organic matter erosion

and decay during topset degradation generally results in substantial increase in the coastal onlap/offlap amplitude, which can result in an overestimation of the sea-level variations. These results are consistent with the discrepancy in sea-level amplitude reconstructions between sequence stratigraphic interpretations and geochemical models based on stable isotopes over the Cretaceous.

MONTCLAIR STATE UNIVERSITY

Coastal Onlap/Offlap Amplification due to Organic Sediment Accumulation and Degradation:
Implications for Sea Level Reconstruction

by

Norjmaa Khosbaatar

A Master's Thesis Submitted to the Faculty of

Montclair State University

In Partial Fulfillment of the Requirements

For the Degree of

Master of Science

August 2021


College of Science and Mathematics

Department of Earth and Environmental Studies

Thesis Committee:


Dr. Jorge Lorenzo-Trueba

Thesis Sponsor


Dr. Sandra Passchier

Committee Member


Dr. Ying Cui

Committee Member

COASTAL ONLAP/OFFLAP AMPLIFICATION DUE TO ORGANIC SEDIMENT
ACCUMULATION AND DEGRADATION: IMPLICATIONS FOR SEA LEVEL
RECONSTRUCTION

A THESIS

Submitted in partial fulfillment of the requirements

For the degree of Master of Science

by

Norjmaa Khosbaatar

Montclair State University

Montclair, NJ

2021

Copyright © 2021 by *Norjmaa Khosbaatar*. All rights reserved.

TABLE OF CONTENTS

1. Introduction.....	1
2. Background.....	2
3. Model Description	5
4. A Dimensionless Form.....	7
5. Model Solution.....	9
6. Modeling Behaviors and Validation.....	10
a. Deltaic evolution not accounting for organic sediment dynamics.....	11
b. Deltaic evolution accounting for organic sediment dynamics.....	12
c. Connecting model results with field observations.....	14
7. Implications for Sea Level Reconstruction.....	15
8. References.....	18
9. Appendix.....	23

FIGURES

Figure 1. (A) Idealized geometry of deltaic evolution in the cross profile. (B) Coastal onlap using sequence stratigraphy. (C) Coastal offlap using sequence stratigraphy. (D) Coastal onlap during sea-level fall. (E) Coastal onlap during sea-level rise. (F) Coastal offlap during sea-level fall.....4

Figure 2. Idealized geometric delta profile with main parameters. Second profile showing shoreline transgression and coastal onlap with a rise in sea-level. Third profile showing a break in geometry after forced transgression.....7

Figure 3. ABT and SH trajectories over time. γ_{rise} is the onlap vertical change and γ_{fall} is the offlap vertical change during each phase of sea-level rise and sea-level fall. ΔZ shows the change in sea-level in each phase.....11

Figure 4. ABT and SH trajectories over time with $P^*=0$ in the solid lines and $P^*=0.5$ in dashed lines. Cf_i and Cf_a values when $P^*=0.5$14

Figure 5. Panel 1 – ABT and SH trajectories of three model runs of $\omega=0.8$ a deltaic prism with $P^*=0.2$, $P^*=0.5$ and $P^*=0.8$. Panel 2 – The values of $\gamma/\Delta Z$ for each run with varying P^* values. The red shaded region shows when there is an underestimation (>1) of sea-level change when using onlap patterns and the white region shows an overestimation (<1) of sea-level change when using onlap patterns.16

TABLES

Table 1. State Variables and their Dimensions.....	8
Table 2. Input parameters and their dimensionless symbols.....	8

1. INTRODUCTION

Fluvio-deltaic environments serve as both home to millions of people and reservoirs for natural resources. Additionally, their associated sediment prisms preserve one of the most complete records of climate, sea level, and tectonics over a large fraction of Earth's history (National Research Council 2012). These records can help us improve our process-based understanding of the driving mechanisms of past sea-level changes, as well as constrain predictions of future sea-level change (Church and Clark 2018, Kopp et al., 2019). Although sea-level changes are often found to represent the most important boundary condition affecting coastal-plain transport systems (Van Wagoner et al., 1990, Van Wagoner 1995, Catuneanu et al., 2009, Blum et al., 2013, Zhang et al., 2019), we still lack a rigorous quantitative theory to reconstruct past sea-level variations from the stratigraphic record. Theories for stratigraphic interpretation need to be adapted to incorporate autogenic (internal) processes that could play a significant role, but are to date largely unexplored (Paola et al., 2009, Hajek & Straub 2017). In particular, *in situ* organic matter accumulation via plant growth has generally received little attention despite accounting for a significant volume fraction of sedimentation in deltaic plains (Kosters et al., 2000; Reddy and DeLaune 2008, Törnqvist et al. 2008, Lorenzo-Trueba et al. 2014). Furthermore, plant matter accumulation on coastal wetlands, which are among the most productive systems in the world (Costanza et al., 1997; Reddy and DeLaune, 2008), has been identified as a potential control of fluvio-deltaic evolution (Fisk, 1960; Meckel et al., 2007; Törnqvist et al., 2008; van Asselen et al., 2009; van Asselen, 2011).

In order to address the relative role of organic sediment dynamics on the stratigraphic evolution of fluvio-deltaic depositional systems, first, we discuss the interplay between the magnitude of sea-level change and organic sediment dynamics, such as coastal onlap/offlap patterns. Second, we extend an existing profile model for the longitudinal profile evolution of a fluvio-deltaic system to incorporate not only organic matter accumulation but also its degradation and decay under sea-level cycles. Finally, we use the resulting model to (1) predict the volume fraction of organic matter preserved in the sedimentary prism and (2) systematically quantify the potential error of sea-level estimates based on stratigraphic indicators for a wide variety of organic sediment accumulation rates and sea-level change scenarios.

2. BACKGROUND

The long profile geometry of fluvio-deltaic environments can be conceptualized in terms of two primary sedimentary environments: the fluvial region or topset, which generally exhibits low topographic relief, and an offshore region or foreset with typically steeper gradients (Figure 1A). The topset is delimited by two geomorphic moving boundaries: the alluvial-basement transition (ABT), where the depositional fluvial region transitions into a bedrock fluvial region, and the shoreline (SH), located at sea level. In sequence stratigraphic theory (e.g., Vail et al. 1977, Van Wagoner et al. 1990), periods of sea-level rise are generally associated with a rise of the topset elevation due to enhanced fluvial deposition, which lead to coastal onlap and transgression (i.e., a landward shift of both the ABT and SH) (Figure 1B). In contrast, periods of sea-level fall are typically associated with topset degradation due to fluvial incision, which lead to coastal offlap and regression (i.e., a seaward shift of both the ABT and SH) (Figure 1C). In both scenarios,

the vertical change in onlap or offlap γ is assumed to be of equal magnitude to the change in sea-level ΔZ (i.e., $\gamma = \Delta Z$).

Although sequence stratigraphic theory provides a broad conceptual framework for evaluating ancient deposits and reconstructing sea level from strata, a number of modeling and experimental studies have shown that the magnitude of coastal onlap and offlap in response to sea-level changes varies between depositional systems and is a function of both allogenic and autogenic (internal) processes (Swenson 2005, Swenson and Muto 2007, Kim and Muto 2007, Paola et al. 2009, Lorenzo-Trueba et al. 2013, Anderson et al. 2019). In other words, the response of fluvio-deltaic environments can be more complicated than what Figures 1B and 1C illustrate. For example, during sea-level fall, a high sediment supply relative to the topset length can result in a geologically long-lived topset aggradation before shifting to degradation (Figure 1D).

We can frame the geometric relationship between the magnitude of coastal onlap and offlap and sea-level change as

$$\gamma = \Delta Z + \alpha \cdot \Delta L, \tag{1}$$

where α is the topset slope, $\Delta L = L_2 - L_1$, L_1 is the topset length at $t = t_1$, and L_2 is the topset length at $t = t_2$ (Figure 1D). Fluvio-deltaic topsets generally exhibit low topographic relief (i.e., $\alpha \sim 1/10,000$) and a sea-level amplitude change is consistent with Quaternary eccentricity-driven eustatic sea level changes (i.e., $\Delta Z \sim 100$ m). Assuming an associated topset length change between highstand and lowstand of $\Delta L \sim 100$ km (using the average continental shelf width as a proxy), we find that the error in the sea-level estimate based on equation 1 would be of ~ 10 m (i.e., $\gamma = \Delta Z + 10$ m). This back of the

envelope calculation emphasizes that the magnitude of coastal onlap and offlap is not only a function of variations in sea-level but also changes in topset length.

Accumulation, degradation and decay of organic matter on the fluvio-deltaic plain can drive significant changes in sediment volume in a fluvio-deltaic prism, which in turn lead to changes in topset length (Lorenzo-Trueba et al. 2012). For instance, an increase in length associated with organic sediment accumulation can result in coastal onlap amplification (i.e., $\gamma_{org} > \gamma$), and therefore a larger departure between the magnitude of coastal onlap and sea-level change (i.e., $\gamma_{org} > \Delta Z > \gamma$) (see Figure 1E). Under topset degradation, however, a significant fraction of the organic sediment volume previously accumulated can erode and decay, which can result in an amplification of coastal offlap change (i.e., $\gamma_{org} > \Delta Z > \gamma$; see Figure 1F). We quantify these dynamics in more detail in the sections below.

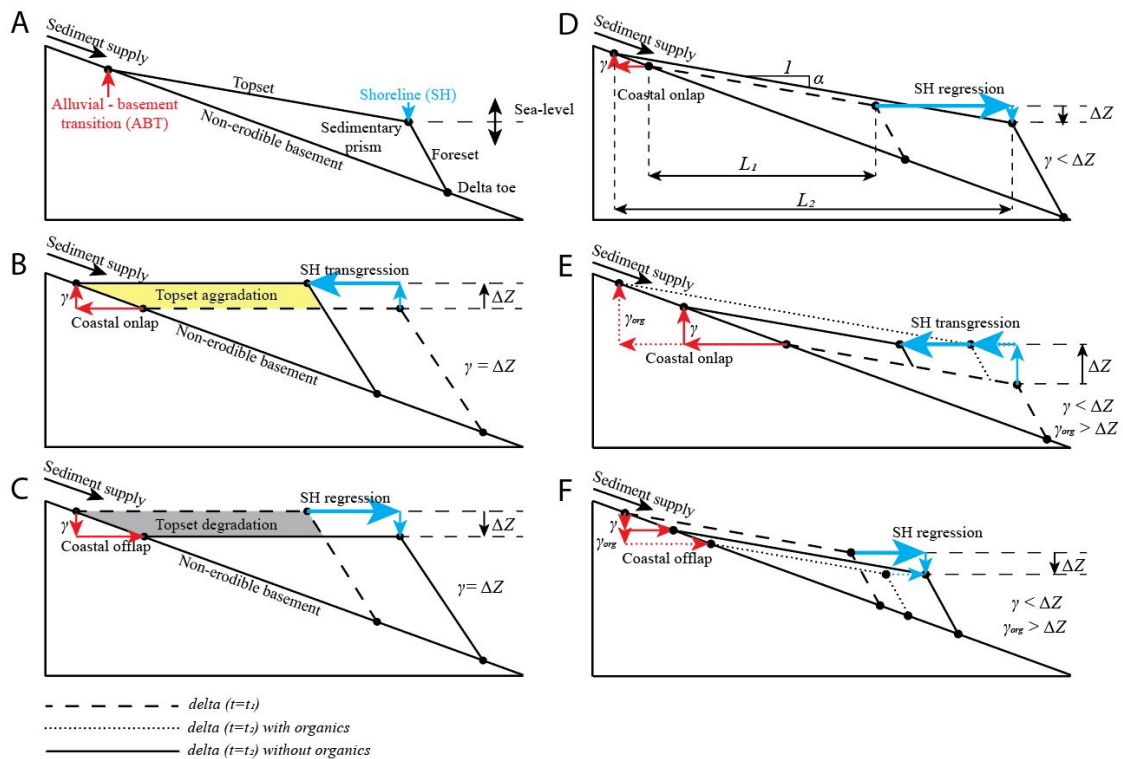


Figure 1: (A) Idealized geometry of deltaic evolution in the cross profile. (B) Coastal onlap using sequence stratigraphy. (C) Coastal offlap using sequence stratigraphy. (D) Coastal onlap during sea-level fall. (E) Coastal onlap during sea-level rise. (F) Coastal offlap during sea-level fall.

3. MODEL DESCRIPTION

To quantify the magnitude of coastal onlap/offlap as a function sea-level change and organic sediment dynamics, we extended a model for the profile evolution of a fluvio-deltaic system (Lorenzo-Trueba et al. 2012) to account for organic matter accumulation, erosion and decay under sea-level level cycles. We define sea-level $Z(t)$ as follows:

$$Z(t) = A \cdot \sin(B \cdot t) \quad (1)$$

where A is the amplitude of sea-level changes and B as the frequency (i.e., 1/period). A key feature of the model is the idealized geometry of the sediment prism, bounded below by a linear basement, and from above by the subaerial topset and the subaqueous foreset (Figure 1).

We compute change in sediment volume of the system as a function of the upstream sediment input from the river q_{in} , the rate of organic matter accumulation ϑ_{org} at any location along the topset, and the rate of erosion and decay of previously deposited organic sediments ϑ_{ero} .

$$\frac{dV}{dt} = q_{in} + \int_R^S \vartheta_{org} \cdot dx + \int_R^S \vartheta_{ero} \cdot dx \quad (2)$$

where $x = R$ is the location of the alluvial-basement transition and $x = S$ is the location of the shoreline (Fig. 2).

Following Lorenzo-Trueba et al. (2012), we describe the rate of organic matter accumulation in terms of the rate of sea-level rise $\dot{Z} = dZ/dt$ and the production of *in situ* organic matter P as follows:

$$\vartheta_{org} = \max(0, (\dot{Z}, P)) \quad (3)$$

When the rate of sea level rise \dot{Z} is larger than the rate of plant production P , riverine sedimentation inundates the resulting space if available; otherwise SH transgression takes place. In contrast, when the rate of sea level rise \dot{Z} is below the rate of plant production P , then the organic sediment excess rapidly decays via aerobic respiration, and only the subaqueous portion of the organic sediment contributes to the sedimentary volume.

We determine the rate of erosion of organic matter based on the geometry of the problem as follows:

$$\vartheta_{ero} = \max\left(0, \dot{Z} - \alpha \cdot \frac{dS}{dt}\right) \cdot C_{fi}(t^*) \quad (4)$$

where C_{fi} is the carbon fraction of the top sediment layer deposited at time t^* , which matches the current time t when there is no prior topset erosion. We define the instantaneous carbon fraction C_{fi} at any point in time t as follows:

$$C_{fi} = \frac{\int_R^S \vartheta_{org} \cdot dx}{q_{in} + \int_R^S \vartheta_{org} \cdot dx} \quad (5)$$

Additionally, we compute the average carbon fraction C_{fa} as follows:

$$C_{fa} = \frac{\int_0^t \left(\int_R^S \vartheta_{org} \cdot dx \right) \cdot dt}{\int_0^t q_{in} \cdot dt + \int_0^t \left(\int_R^S \vartheta_{org} \cdot dx \right) \cdot dt} \quad (6)$$

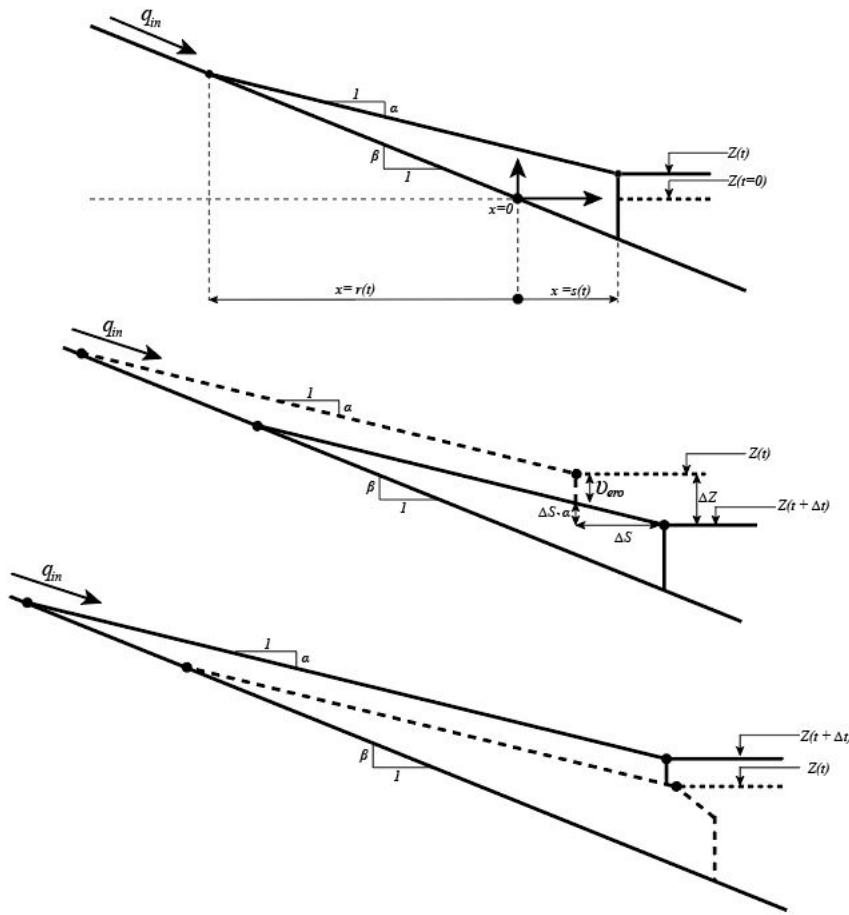


Figure 2: Panel A shows the idealized geometric delta profile with main parameters. Panel B shows shoreline transgression after sea-level fall with topset degradation. Panel C depicts shoreline regression after sea level rise.

4. A DIMENSIONLESS FORM

We rewrite the use dimensionless variables in order to reduce the number of controlling parameters. For dimensions with length, we use a characteristic basin length l of 100 km. For the slope of the basement β , and the topset α , we use realistic ratios found in the field. Our dimensionless variables are:

$$A^* = \frac{A}{l\beta}, P^* = \frac{Pl}{q_{in}}, t^* = \frac{t}{\tau}, R^* = \frac{R}{l}, S^* = \frac{S}{l}, Z^* = \frac{Z}{l\beta}, L^* = \frac{L}{l} \quad (7)$$

With the definitions in (7), and dropping the * superscript for convenience of notation, the dimensionless governing equation under sea-level cycles becomes:

$$\frac{dV}{dt} = 1 + \int_R^S \vartheta_{org} \cdot dx + \int_R^S \vartheta_{ero} \cdot dx \quad (8)$$

Tables 1 and 2 are lists of the state variables and their dimensions with associated dimensionless symbol and the input parameters for the numerical model. Values of A are dimensionless amplitudes which can range from 0 to 1, which relate to sea-level amplitudes of 30 m to 100 m in amplitude. We use a dimensionless frequency B value of 1 which corresponds to a period of 100,000 years.

Table 1

State Variables and their Dimensions

Symbol	Units	Description
t	T	Time
x	L	Horizontal distance
R	L	Alluvial-basement transition horizontal distance from origin
S	L	Shoreline horizontal distance from origin
η (<i>eta</i>)	L	Sediment height above basement
V_{in}	L ²	Volume of inorganic sediment supply
V_{org}	L ²	Volume of organic sediment supply
Z	L	Sea-level curve

Table 2

Input parameters and their dimensionless symbols

Symbol	Units	Description
--------	-------	-------------

q_{in}	$L^2 \cdot T^{-1}$	Inorganic sediment flux at ABT
β	-	Basement slope
α	-	Topset slope
P	L/T	Rate of plant production

5. MODEL SOLUTION

We discretize in space using n nodes with a uniform step size Δx , where $i=1$ represents the most landward node, and $i=n$ represent the most seaward node. We discretize time with a uniform time step of Δt , where $t_j = j\Delta t$. The sedimentary wedge develops from the origin $x=0$, which we have chosen to be the initial intersection of the base-level with the non-erodible basement. The origin is at the interface of two nodes in the center of the domain.

At $t=0$, we set the initial ABT and SH conditions to be at the origin, i.e., $R(0) = S(0) = 0$. Our model determines the ABT and SH trajectories at each time step by making an initial estimate of the SH location, and then updating this estimate to ensure that mass is conserved in the delta. In more detail, at a given time step $t_j > 0$, we select a guess for the SH location as:

$$S_j = S_{j-1} + \Delta x \quad (9)$$

Using our linear geometry, we can calculate the ABT location $R(j)$ as:

$$R_j = -\frac{\alpha}{(\beta-\alpha)} \cdot \left(\frac{S_j+Z}{\beta}\right) - \left(\frac{Z}{\beta}\right) \quad (10)$$

We can then calculate the total sedimentation deposited within our domain in each cell, through time

$$\eta_{j+1} \begin{cases} Z + \alpha \cdot (S - x_i) + x_i \cdot \beta, & R_j > x_i > S_j \\ \eta_j, & \text{otherwise} \end{cases} \quad (11)$$

Then the estimated total volume of the sedimentation in the system is

$$V_j = \Delta x \sum_{i=1}^n \eta_{i,j} \quad (12)$$

In order to ensure the mass is conserved at every time step, we compare the numerically calculated volume of the delta with the expected analytical volume (V_T and V_j). If the difference between these two values is within a certain tolerance, then the model moves onto the next time step. Otherwise, we use the difference between the two volumes to update the guess of the SH location as:

$$s_j = s_j + \phi \cdot (V_T(t_j) - V_j) \quad (13)$$

where $\phi = 0.005$ is a relaxation parameter. With a new guess for the SH location we can follow again the steps described by equations above. We repeat this sequence until we converge to a solution in which the difference between V_T and V_j is below 10^{-3} .

We plot the ABT and SH over dimensionless time in the vertical and a dimensionless distance in the horizontal axis, shown in Figure 3a.

6. MODELING BEHAVIORS AND VALIDATION

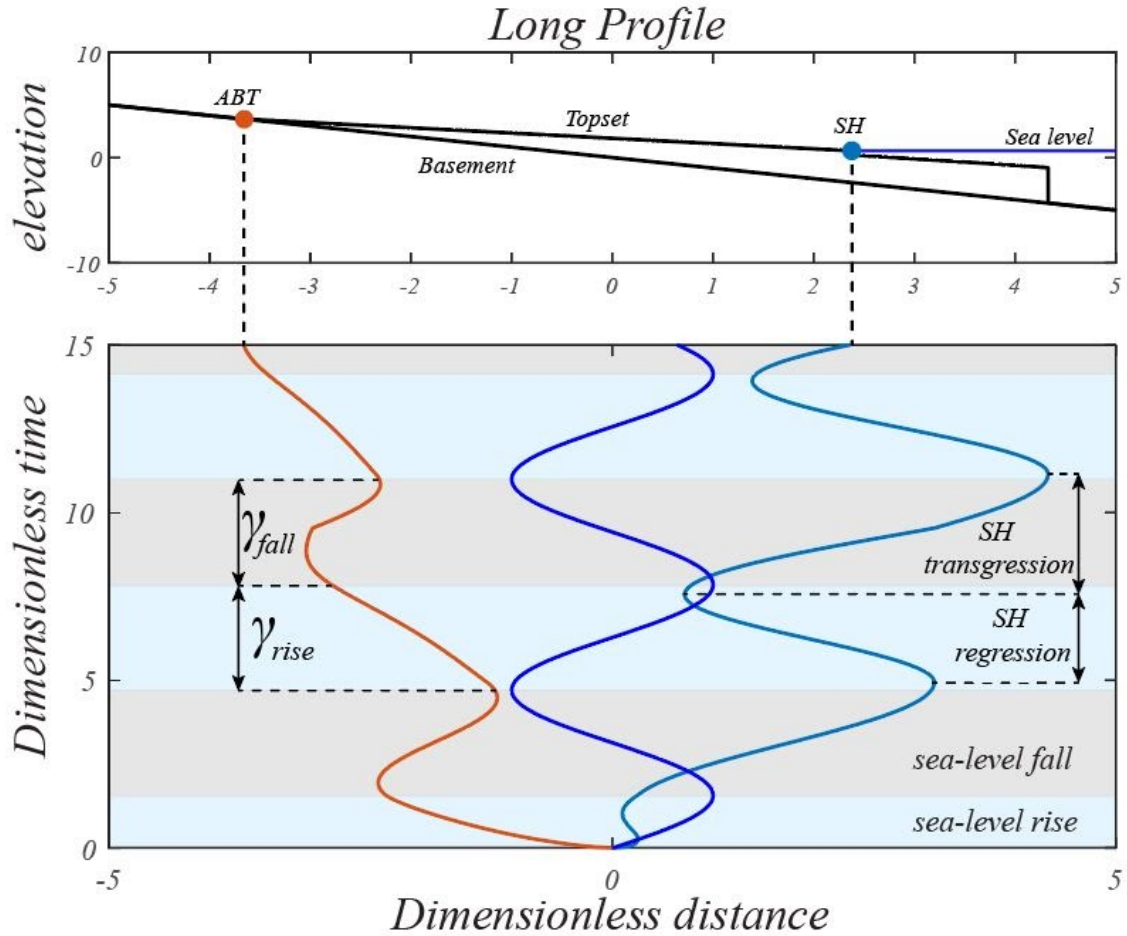


Figure 3: ABT and SH trajectories over sea level cycles with $Z = A \sin (B \cdot t)$. Onlap occurs when the ABT migrates left of the origin (landward), and offlap occurs when the ABT migrates right of the origin (seaward). SH transgression and regression occurs when the SH migrates right of the origin (seaward) and left of the origin (landward) respectively.

a. *Deltaic evolution not accounting for organic sediment dynamics*

In order to determine how the sedimentary prism behaves under sea-level cycles without the addition of *in situ* organic matter, we analyze how the trajectories of the ABT and the SH behave with respect to sea level variations and a sloped fluvial surface. The

main external factors that influence onlap and offlap are sediment supply, the length of the fluvial topset and the topset slope. In figure 3, we see that the modeling behaviors suggest that the response of the ABT is susceptible to time lags during sea-level cycles, particularly during sea-level fall, where the ABT can continue to undergo coastal onlap for a portion of the sea-level fall phase. This occurs when the sloped length of the fluvial topset is long enough and that the effect of sea-level fall does not instantaneously affect the moving boundary. This suggests that without organic sediment dynamics, the onlap and offlap patterns can cause a discrepancy from stratigraphic interpretation since the movement of the ABT is not directly related to the instantaneous change in sea-level.. The migration of the SH is also affected, although not as much as the ABT by sea level cycles. The onset of SH transgression occurs at the end of the highstand phase until the start of the lowstand phase, and the onset of SH regression occurs at the start of the highstand phase as shown in Figure 3.

b. *Deltaic evolution accounting for organic sediment dynamics*

Figure 4 highlights the different ABT and SH trajectories of a deltaic prism with inorganic sedimentation and a deltaic prism with the inclusion of organic sedimentation. There is an asymmetry of organic sediment accumulation and degradation over time, which alters both the responses of the ABT and SH. The response of the ABT is amplified, and the SH is dampened. The additional sedimentation from organic matter production results in accumulation and preservation if conditions allow, which contributes to the overall volume. This influx of organic sedimentation creates a larger delta during the topset aggradation phase and allows for further progradation of the SH during a sea level rise phase. The length of the fluvial surface increases in response to the

increase in sedimentation. This progradation of the SH is extended due to the accommodation being filled in by both the *in situ* plant production on the fluvial surface, and the inorganic sediment flux to the foreset region thus the combined volume allows the SH to keep pace with sea-level rise for longer than a scenario with no organic matter sedimentation. During a transgression, the vertical aggradation is larger due to the *in situ* organic sedimentation, which produces a slower migration of the shoreline landward, and a further migration of the ABT landward as a result of the lengthening of the fluvial topset. The amplification of the ABT response to sea-level changes when P^* increases is caused by the accumulation of organic matter during topset aggradation, and the reduction of organic matter during topset degradation. Given additional sediment via organic matter, the deltaic fluvial length expands further.

In the case of topset degradation, any exposed organic sedimentation is either exported from the system or decomposed. Therefore, the ABT undergoes coastal offlap and migrates further seaward compared to a scenario with no organic matter sedimentation. Degradation of the fluvial surface also causes a faster decrease in overall deltaic volume and a shortening of the length of the fluvial topset, since inorganic sedimentation is preserved within the geometry under sea-level fall but organic sedimentation is not. Therefore, the trajectory of the ABT is amplified as we increase P^* as shown in Figure 4.

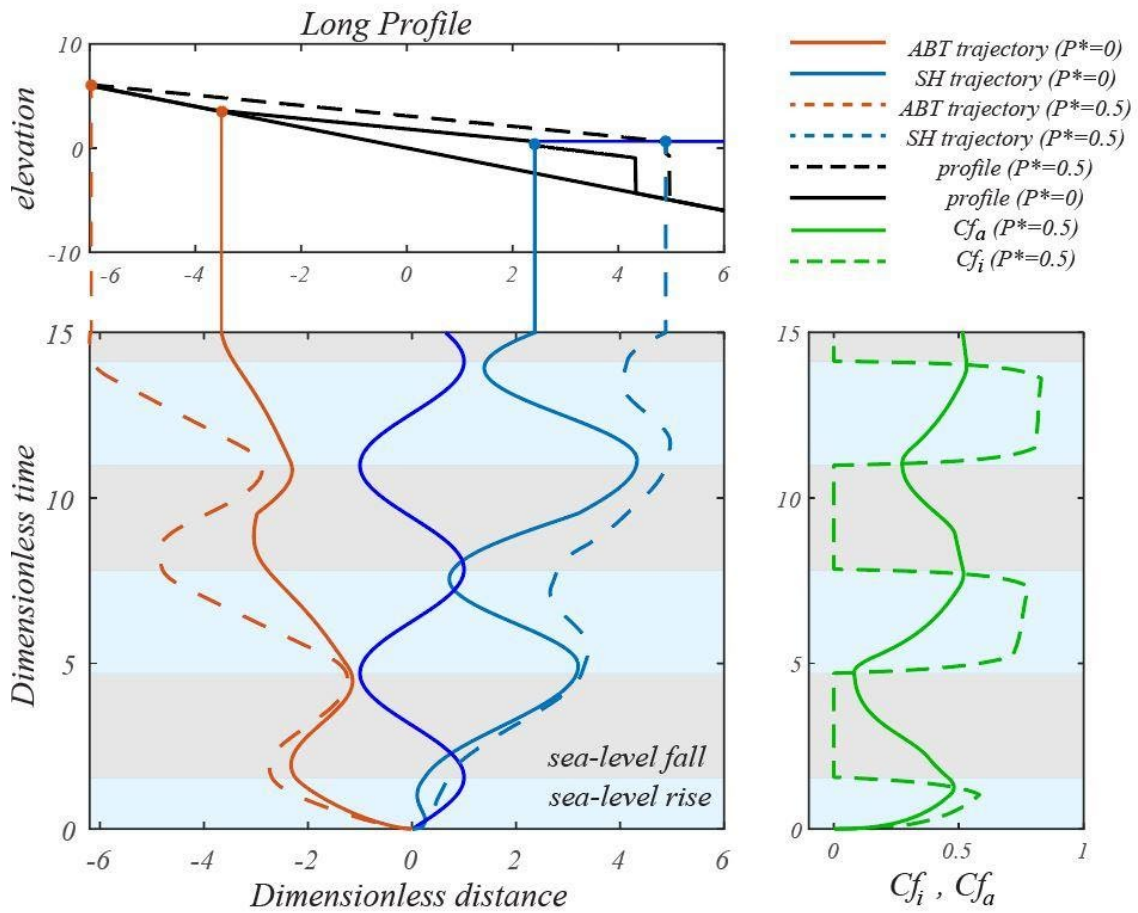


Figure 4: ABT and SH trajectories over time with $P^*=0$ in the solid lines and $P^*=0.5$ in dashed lines. Cf_i and Cf_a values when $P^*=0.5$.

c. Connecting model results with field observations

We calculate the instantaneous and average carbon fraction, explained above to compare to coal literature in order to validate our model outputs. Coal geologists have noted that the most significant coal accumulation occurs when the ratio of the rate of accommodation via base-level A is close to the rate of *in situ* plant production P (Bohacs and Sutter, 1997). In figure 4, we calculate the instantaneous carbon fraction Cf_i and average carbon fraction Cf_a over sea-level cycles. The values of Cf_i are related to the rate

of change in sea-level and the ratio of the *in situ* plant production and total sedimentation (organic and inorganic) at every time step. In the plot above we have the rate of plant production at $P^*=0.5$ and the rate of accommodation of $A=1$, where we observe the peaks in Cf_i when the rate of accommodation is near the rate of plant production (0.5). When the rate of sea-level rise is at its highest, the Cf_i values plateau since the limiting factor is the rate of plant production, and its inability to keep pace with the increase in accommodation space. During phases of sea-level fall, we see Cf_i values of 0 since there is no accommodation available in the subaqueous region. We also calculate the average carbon fraction Cf_a which looks at the bulk ratio of the instantaneous carbon fraction over time. Since this is accounting for previous deposits of organic material, the Cf_a values do not reach 0 during sea-level fall. During the sea-level rise phases, the peak of Cf_a values are towards the end of the highstand phase.

7. IMPLICATIONS FOR SEA LEVEL RECONSTRUCTION

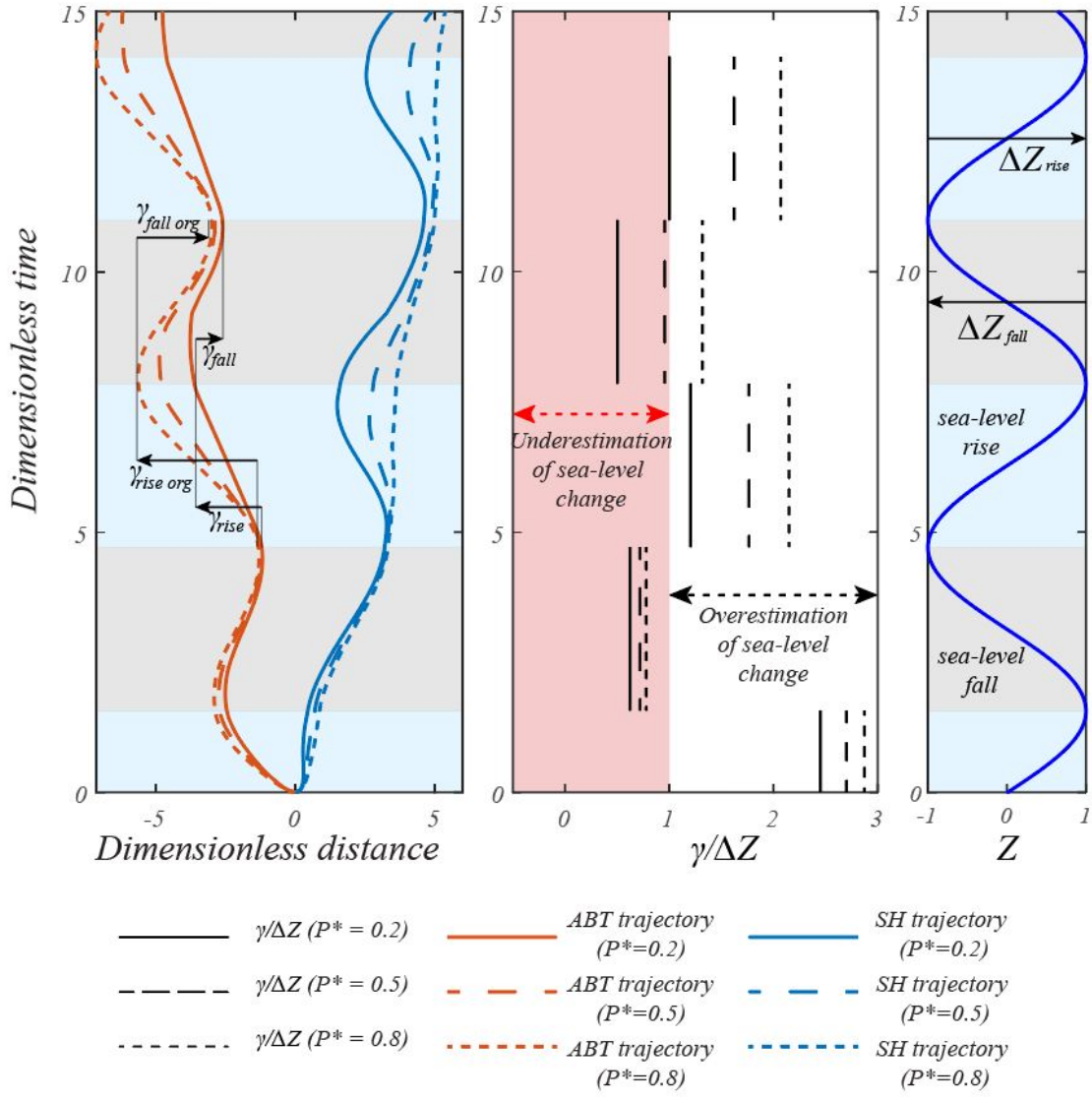


Figure 5: Panel 1 – ABT and SH trajectories of three model runs of variety of P^* values. a deltaic prism with $P^* = 0.2$, $P^* = 0.5$ and $P^* = 0.8$. Panel 2 – The values of $\gamma/\Delta Z$ for each run with varying P^* values. The red shaded region shows when there is an underestimation (>1) of sea-level change when using onlap patterns and the white region shows an overestimation (<1) of sea-level change when using onlap patterns.

In this section we quantify the error between the magnitude of coastal onlap/offlap vertical change γ relative to the magnitude of sea-level change ΔZ (Figure 5). In

particular, we plot the ratio $\gamma/\Delta Z$ and the ABT and SH trajectories for different rates of plant production P^* . We find using onlap/offlap patterns tends to overestimate the magnitude of sea-level change (i.e., $\gamma/\Delta Z > 1$), but underestimations can also occur (i.e., $\gamma/\Delta Z < 1$). Moreover, the tendency to overestimate the amplitude of sea-level oscillations increases as we increase P^* .

These results imply that sea-level reconstructions based on coastal onlap/offlap patterns (Vail 1977, and Haq 2014) of periods associated with high rates of coal accumulation such as the Carboniferous or the Cretaceous can significantly overestimate the amplitude of the sea-level oscillations. These results are consistent with recent compilations of sea-level reconstructions over the Cretaceous (e.g., Simmons et al. 2020), which include estimates from Haq et al. 2014 with amplitudes ~ 130 meters, substantial larger than the rest (e.g., Miller et al. 2005, with amplitudes ~ 40 meters).

Overall, this work emphasizes the importance of accounting for organic sediment dynamics on the evolution of fluvial-deltas. Future work will aim to more directly couple the modeling framework and results presented here with field data from different periods in the geologic past, from high to low rates of organic matter accumulation, to better understand the effect of organic sediment dynamics on paleo sea-level reconstruction.

8. REFERENCES

- Anderson, W., Lorenzo-Trueba, J. and Voller, V., 2019. A geomorphic enthalpy method: Description and application to the evolution of fluvial-deltas under sea-level cycles. *Computers & Geosciences*, 130, pp.1-10.
- Blum, M., Martin, J., Milliken, K., Garvin, M., 2013. Paleo valley systems: insights from Quaternary analogs and experiments. *EarthSci. Rev.* 116,128–169.
<https://doi.org/10.1016/j.earscirev.2012.09.003>.
- Bohacs, K. M., and J. Suter (1997), Sequence stratigraphic distribution of coaly rocks; fundamental controls and paralic examples, *AAPG Bull.*, 81, 1612–1639
- Catuneanu, O., Abreu, V., Bhattacharya, J.P., Blum, M.D., Dalrymple, R.W., Eriksson, P.G., Fielding, C.R., Fisher, W.L., Galloway, W.E., Gibling, M.R. and Giles, K.A., 2009. Towards the standardization of sequence stratigraphy. *Earth-Science Reviews*, 92(1-2), pp.1-33, doi:10.1016/j.earscirev.2008.10.003
- Church, J.A., P.U. Clark, A. Cazenave, J.M. Gregory, S. Jevrejeva, A. Levermann, M.A. Merrifield, G.A. Milne, R.S. Nerem, P.D. Nunn, A.J. Payne, W.T. Pfeffer, D. Stammer and A.S. Unnikrishnan, 2013: Sea Level Change. In: *Climate Change 2013: The Physical Science Basis. Contribution of Working Group I to the Fifth Assessment Report of the Intergovernmental Panel on Climate Change* [Stocker, T.F., D. Qin, G.-K. Plattner, M. Tignor, S.K. Allen, J. Boschung, A. Nauels, Y. Xia, V. Bex and P.M. Midgley (eds.)]. Cambridge University Press, Cambridge, United Kingdom and New York, NY, USA.
- Costanza, R., et al. (1997), The value of the world's ecosystem services and natural capital, *Nature*, 387, 253–260, doi:10.1038/387253a0.

Fisk, H. N. (1960), Recent Mississippi River sedimentation and peat accumulation, in *Congress pur l'avancement des études de stratigraphie et de géologie du Carbonifère*, pp. 187–199, *Compte Rendu*, Heerlen, Netherlands

Hajek, E.A., Straub, K.M., 2017. Autogenic sedimentation in clastic stratigraphy. *Annu. Rev. Earth Planet Sci.* 45, 681-709. <https://doi.org/10.1146/annurev-earth-063016-015935>.

Haq, B.U. and Schutter, S.R., 2008. A chronology of Paleozoic sea-level changes. *Science*, 322(5898), pp.64-68.

Haq, B.U., 2014. Cretaceous eustasy revisited. *Global and Planetary change*, 113, pp.44-58.

Johnson, M.E., 2010, Tracking Silurian eustasy: alignment of empirical evidence or pursuit of deductive reasoning? *Palaeogeography, Palaeoclimatology, Palaeoecology*, 296: 276-284.

Kim, W., and T. Muto (2007), Autogenic response of alluvial-bedrock transition to base-level variation: Experiment and theory, *J. Geophys. Res.*, 112, F03S14, doi:10.1029/2006JF000561.

Kopp, R.E., Gilmore, E.A., Little, C.M., Lorenzo-Trueba, J., Ramenzoni, V.C. and Sweet, W.V., 2019. Usable science for managing the risks of sea-level rise. *Earth's Future*, 7(12), pp.1235-1269.

Kosters, E.C., VanderZwaan, G.J. and Jorissen, F.J., 2000. Production, preservation and prediction of source-rock facies in deltaic settings. *International journal of coal geology*, 43(1-4), pp.13-26.

Lorenzo-Trueba, J., Voller, V.R., Paola, C., Twilley, R.R. and Bevington, A.E., 2012. Exploring the role of organic matter accumulation on delta evolution. *Journal of Geophysical Research: Earth Surface*, 117(F4), doi:10.1029/2012JF002339

Lorenzo-Trueba, J., Voller, V.R. and Paola, C., 2013. A geometric model for the dynamics of a fluvially dominated deltaic system under base-level change. *Computers & Geosciences*, 53, pp.39-47, doi:10.1016/j.cageo.2012.02.010.

Lorenzo-Trueba, J. and Ashton, A.D., 2014. Rollover, drowning, and discontinuous retreat: Distinct modes of barrier response to sea-level rise arising from a simple morphodynamic model. *Journal of Geophysical Research: Earth Surface*, 119(4), pp.779-801, doi:10.1002/2013JF002941.

Meckel, T. A., U. S. Ten Brink, and S. J. Williams (2007), Sediment compaction rates and subsidence in deltaic plains: Numerical constraints and stratigraphic influences, *Basin Res.*, 19, 19–31, doi:10.1111/j.1365-2117.2006.00310.x

Miller, K.G. and Mountain, G.S., 1996. Drilling and dating New Jersey Oligocene-Miocene sequences: Ice volume, global sea level, and Exxon records. *Science*, 271(5252), pp.1092-1095.

Miller, K.G., Kominz, M.A., Browning, J.V., Wright, J.D., Mountain, G.S., Katz, M.E., Sugarman, P.J., Cramer, B.S., Christie-Blick, N. and Pekar, S.F., 2005. The Phanerozoic record of global sea-level change. *science*, 310(5752), pp.1293-1298.

Miller, K.G., Browning, J.V., Mountain, G.S., Sheridan, R.E., Sugarman, P.J., Glenn, S. and Christensen, B.A., 2014. History of continental shelf and slope sedimentation on the US middle Atlantic margin. *Geological Society, London, Memoirs*, 41(1), pp.21-34.

Paola, C., Straub, K., Mohrig, D. and Reinhardt, L., 2009. The “unreasonable effectiveness” of stratigraphic and geomorphic experiments. *Earth-Science Reviews*, 97(1-4), pp.1-43.

Reddy, R., and R. D. DeLaune (2008), *Biogeochemistry of Wetlands: Science and Applications*, CRC Press, Boca Raton, Fla., doi:10.1201/9780203491454.

Spasojevic, S., Liu, L.J., Gurnis, M., and Müller, R.D., 2008, The case for dynamic subsidence of the U.S. east coast since the Eocene. *Geophysical Research Letters*, 35, article #, L08305: 6 pp, <https://doi.org/10.1029/2008GL033511>.

Swenson, J.B., Paola, C., Pratson, L., Voller, V.R., Murray, A.B., 2005. Fluvial and marine controls on combined subaerial and subaqueous delta progradation: morphodynamic modeling of compound-clinof orm development. *J. Geophys. Res. Earth Surf.* 110, 1–16. <https://doi.org/10.1029/2004JF000265>.

Swenson, J.B., Muto, T., 2007. Response of coastal plain rivers to falling relative sea-level: allogenic controls on the aggradational phase. *Sedimentology*

Törnqvist, T. E., D. J. Wallace, J. E. A. Storms, J. Wallinga, R. L. Dam, M. Blaauw, M. S. Derksen, C. J. W. Klerks, C. Meijneken, and E. M. A. Snijders (2008), Mississippi Delta subsidence primarily caused by compaction of Holocene strata, *Nat. Geosci.*, 1, 173–176, doi:10.1038/ngeo129

Vail, P.R., Mitchum Jr, R.M. and Thompson III, S., 1977. Seismic stratigraphy and global changes of sea level: Part 4. Global cycles of relative changes of sea level.: Section 2. Application of seismic reflection configuration to stratigraphic interpretation.

van Asselen, S., E. Stouthamer, and T. van Asch (2009), Effects of peat compaction on delta evolution: A review on processes, responses, measuring and modeling, Earth Sci. Rev., 92, 35–51, doi:10.1016/j.earscirev.2008.11.001.

van Asselen, S. (2011), The contribution of peat compaction to total basin subsidence: Implications for the provision of accommodation space in organic-rich deltas, Basin Res., 23, 239–255, doi:10.1111/j.1365-2117.2010.00482.x.

Van Wagoner, J.C., Mitchum, R.M.J., Campion, K.M., Rahmanian, V.D., 1990. Siliclastic sequence stratigraphy in well logs, cores and outcrops. AAPG Methods Explor. Ser. 7, 1-55.

Van Wagoner, J.C., Bertram, G.T., 1995. Sequence stratigraphy of foreland basin deposits. Memoir 64, 487.

9. APPENDIX

